Study of the properties of La-doped ZnS thin Films synthesized by Sol-gel method

Amel Tounsi[1], Djahida Talantikite-Touati[1,3*], Hamid Merzouk[2,3], Hadjira Haddad[1], Roumaïssa Khalfi[1]

[1]*Department of Chemistry, Abderrahmane Mira University, 06000 Bejaia, Algeria*
[2]*Department of Physic, Abderrahmane Mira University, 06000 Bejaia, Algeria*
[3]*LGE Laboratory, Abderrahmane Mira University, 06000 Bejaia, Algeria*

*Corresponding author

DOI: 10.5185/amlett.2018.1963
www.vbripress.com/aml

Abstract

The thin layers of undoped ZnS and ZnS doped La with different concentrations (2, 4, 6, 8 and 10%) were deposited on glass substrates using sol-gel and dip-coating methods. The structural characterization of these samples was carried out by the X-rays diffraction (XRD), scanning electron microscopy (SEM) and atomic force microscopy (AFM). UV-visible and Fourier Transform Infrared spectroscopy (FTIR) have been used to study the effect of dopant on the optical properties of ZnS doped La thin films. Atomic force microscopy images of the films have revealed homogeneous and granular structure and the SEM micrographies show a deposit films with uniform and porous structure. The optical transmission spectra in the UV - visible range have shown that all the doped films present a good optical transmission in the visible domain. Copyright © 2018 VBRI Press.

Keywords: ZnS doped La, nanoparticles, thin films, sol-gel method, UV-visible, SEM.

Introduction

The doped semiconductors were in huge expansion worldwide thanks to their optical and electric properties. They have a wide range of applications such as biosensors and gas sensors [**1,2**], catalysts and photocatalysts [**3,4**], electroluminescent and photo-luminescent phosphors devices [**5,6**], optoelectronic and photovoltaic applications [**7,8**]. Among these materials, zinc sulfide (ZnS) is a well-known optical semiconductor material of important II-VI group transition metal sulfides with a wide band gap (3.7 eV) at room temperature and a high field transmittance in the visible domain [**9,10**]. Furthermore, ZnS has a specific physical characteristics, such as high refraction index [**11**].

Various physical and chemical methods are used to prepare ZnS thin films, such as chemical bath deposition [**12**], RF magnetron sputtering [**13**], pulsed laser deposition PLD [**14**], hydrothermal method [**15**], spray pyrolysis [**16**] and sol-gel [3,11]. The sol-gel technique is one of the most preferred method because the facility of using and it's based on hydrolysis and condensation reactions to form a wet-gel structure. This method has been extended to the fabrication of thin and thick films on different substrates [**17, 18**].

Since the work of Bhargava et al. [**19**] about remarkable optical properties of Mn-doped ZnS nanoparticles that were prepared by a room temperature chemical process in 1994, several studies were reported in literature on doping ZnS with 3d transition metal and rare earth (RE) [3,6,20,21] ions, in order to improve luminescent properties of zinc sulfide.

We have not found in literature, a studies about La-ZnS thin films elaborated by sol-gel technique. For this reason, we have chosen to present in this work the doping of ZnS by the lanthanum. We studied the effect of La-doping on the structural and optical properties of ZnS films and we present the preparation and the characterization of ZnS and La doped ZnS thin films. So, the thin layers of La doped ZnS with different compositions (1-x) ZnS + xLa (x= 0; 2; 4; 6; 8 and 10%) were deposited on glass substrates by a dip-coater using sol-gel method. The structural properties were carried out by the X-ray diffraction (XRD), scanning electron (SEM) and atomic force (AFM) microscopies. The Fourier transform infrared measurements were used to confirm the formation of ZnS bonds and identify any adsorbed species on the crystallite surface. UV-visible spectroscopy at room temperature was used for the optical investigation.

Experimental

ZnS doped La thin films with different concentrations (0, 2, 4, 6, 8 and 10%) are prepared by following steps: zinc acetate dihydrate $Zn(CH_3COO)_2.2H_2O$ (0.1M) and lanthanum III nitrate hexahydrate $(La(NO_3)_3.6H_2O)$ (0.1M) are firstly dissolved in propanol-1. Thiourea CH_4N_2S (0.3M) was dissolved in propanol-1 separately by stirring (300 rpm) at room temperature. Triethanolamine (TEA) was added to the first solution drop by drop. Then, a solution of NaOH (3M) was added to adjust the pH at 12 and to obtain an homogeneous transparent solution. Finally, the solution of thiourea was added to this solution and mixed in the same flask. A constant agitation is maintained during 2 hours, at 300 rpm. Thin films of ZnS doped La were deposited on properly cleaned glass substrates by dip-coating with a velocity of 170 $cm.s^{-1}$. We repeated this step 10 times. Finally, the deposited films were dried at 423 K to remove the mixed solvent and organic substances such as C, H and N.

In order to study the effect of dopant concentration on the optical properties of ZnS doped La thin films, the structural characterization of these samples were carried out at room temperature by X-ray diffraction (XRD) analyses using a powder diffractometer (Expert Pro Panalytical), with CuK_{α} radiation ($\lambda = 1.54051$ *Å*) at 40 *kV* and silicon as internal standard.. The morphology of the films was examined by scanning electron microscopy (SEM Quanta 200, FEI France). The AFM measurements were performed to analyze the surface topography of the layers scanned over the area of 20 μm × 20 μm by three-dimensional (3D) and two dimensional (2D) atomic force microscopy (AFM, Asylum research, MFP 3D classic). IR spectra of samples were recorded with the FTIR (Iraffinity-1 Shimadzu) between 400 and 4000 cm^{-1}. The transmittance was performed with the UV–VIS spectrophotometer (UV-1800 Shimadzu) in the wavelength range 200–800 *nm*.

Results and discussion

Fig. 1 shows the XRD patterns of $ZnS:La^{3+}$ thin films deposited on glass substrate. The spectra were recorded in 2θ between 20° and 80 °. The analyses reveal that the thin layers worked out are amorphous and no peak were detected for all the compositions (x= 0; 2;4;6:8 and 10 %). This result was expected. Indeed, thin films produced by sol-gel method and dip-coating give an amorphous compound [11] and it has been explained by highly disordered present within deposit materials and very small grain sizes [**22**]. A sintering of La-ZnS thin films carried out at 500°C in air during 2 hours, give us a characteristic phase of ZnO. This behavior has been observed by many authors [**23,24**] who report the oxidation of ZnS to ZnO in the presence of air oxygen. So, the achievement of the crystalline phase of ZnS films is possible with a heat treatment under controlled atmosphere [11].

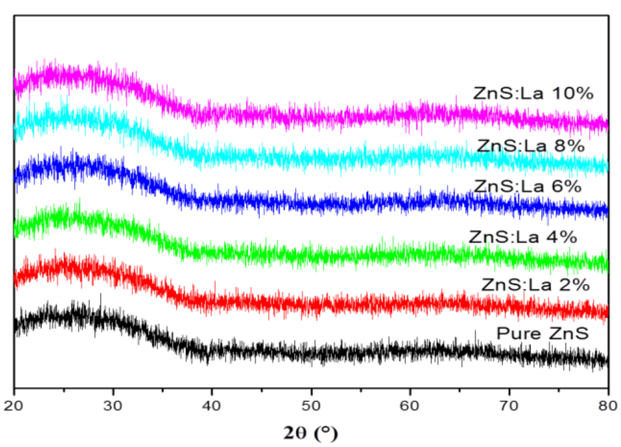

Fig. 1. X-ray diffraction (XRD) spectra of ZnS:La thin films (0-10%).

The FITR analyses confirmed the presence of ZnS. All the spectra observed on the **Fig. 2** of the transmittance spectra of ZnS:La show only one intense peak at 668 cm^{-1} which is attributed by several authors at the Zn-S vibration band [25,26].

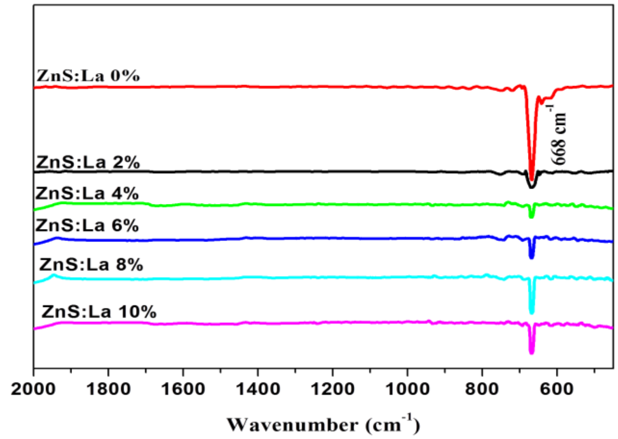

Fig. 2. FTIR spectra of ZnS: La thin films with different compositions (0-10%).

Fig. 3 shows micrographies of the different compositions of $ZnS:La^{3+}$ (0, 4, 6, 8 and 10%) at room temperature. Pure ZnS has some bright spots scattered on the surface which are a crystalline ZnS particles (Yining Zhang). The composition of 4% shows that the surface is covered with grains-shaped corolla which has the phosphorescent edge and center. Clusters of different sizes and shapes are given by the sample of 6%, and the sample of 8% is formed by a long and hexagonal grain shapes. The composition of 10% has a uniform and homogeneous deposition.

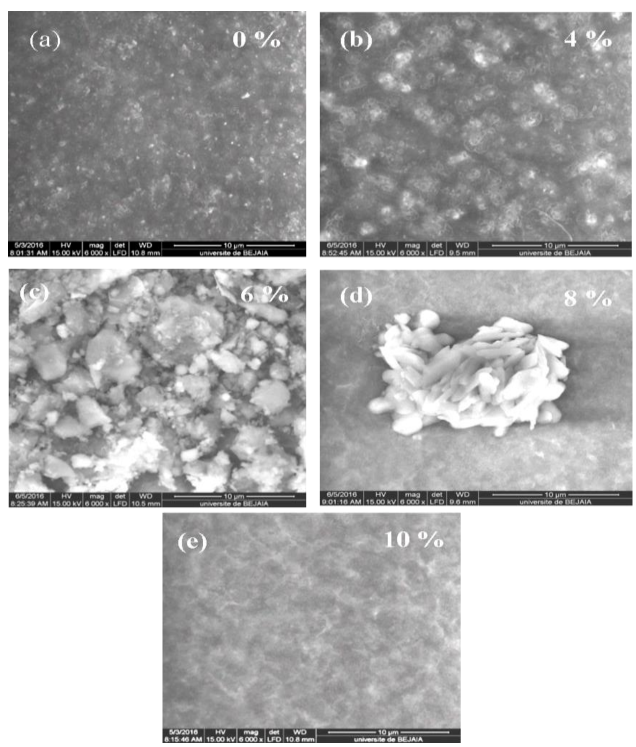

Fig. 3. The SEM micrographs of different compositions of ZnS:La (0-10%).

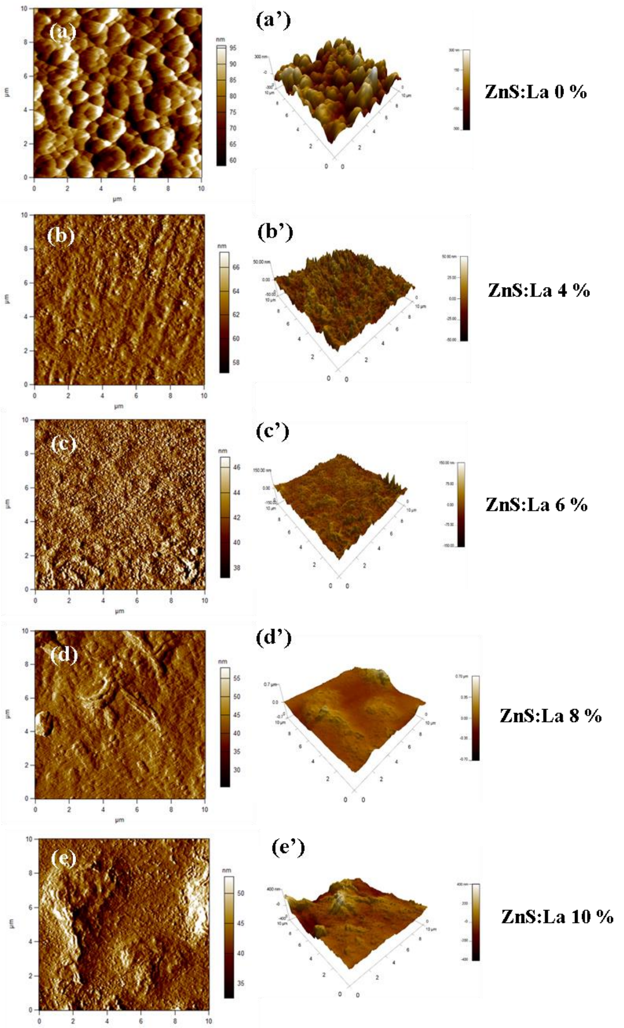

Fig. 4. AFM images 2D (a, b, c, d, e) and 3D (a’,b’,c’,d’, e’) of thin films ZnS:La (0- 10%).

Fig. 4 shows the surface morphology of the thin films of (1-x)ZnS-xLa compositions (x=0, 2, 4, 6, 8 and 10%), deposited on glass substrate at two dimensional (2D).Thin film of pure ZnS shows no planar surface with an important root mean square (RMS) of roughness values (surface roughness). These pictures showed clearly that the surface sample of ZnS:La^{3+} is more homogeneous and less rough compared with a pure ZnS. The surface of La-ZnS layers is formed by small grains that are uniformly distributed. Doping decreases roughness and the obtained values of RMS (nm) are 90.504; 82.19; 12.331; 79.848; 69.665 for respectively 0; 4; 6; 8 and 10 %. The three-dimensional AFM image shows a nanometric grain size with a colonnaire shape.

The optical properties of the zinc sulfide doped lanthanum (ZnS:La^{3+}) thin films were determined from transmittance measurements in the range of 200-1100 nm at room temperature. **Fig. 5** shows the transmittance spectra of ZnS:La^{3+} thin films according to the wavelength. The behavior of curves shows a good homogeneity of deposits ZnS:La thin films. All the composition (1-x)ZnS-xLa have a good transparency in the visible domain(over 50 %). The maximum absorption is observed as shoulders on the curves between 300 and 450 nm for all doped compositions. The UV-visible absorption curves of zinc sulfide doped lanthanum thin films are represented in **Fig. 6**. We observed a considerable increase on the wavelength absorption edge for the (1-x)ZnS-xLa compositions compared to pure ZnS. In the other hand, a blue shift is obtained for the pure ZnS thin film compared with the bulk form which gives in the literature at 345 nm. The absorption threshold is obtained from the intercept of the straight-line portion of the absobance (A) vs the wavelength (λ). The gap is calculated using the formula:

$$Eg = h\nu = hc / \lambda$$

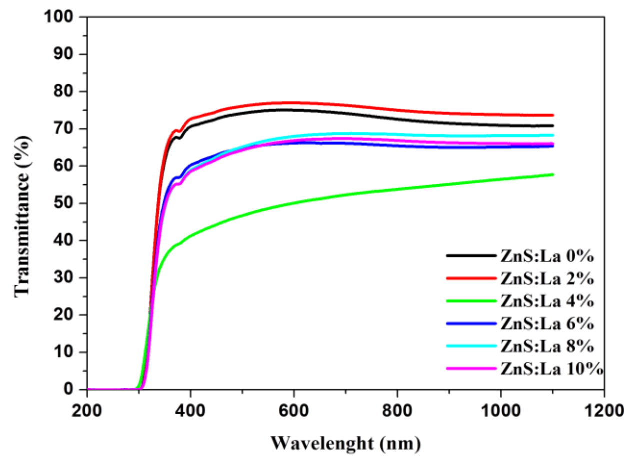

Fig. 5. Optical Transmistance spectra of thin films ZnS:La (0- 10%).

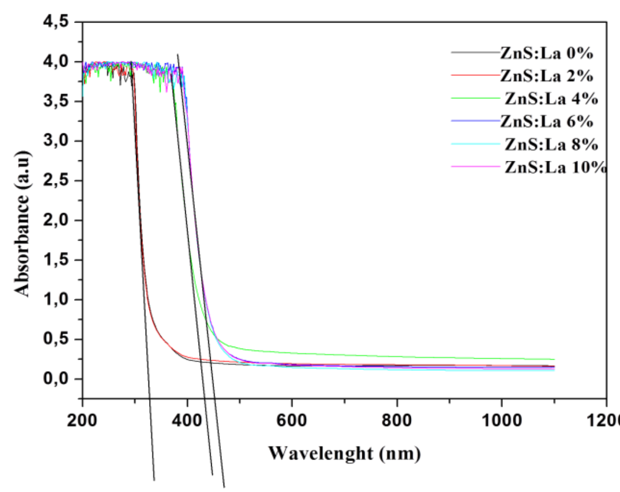

Fig. 6. Optical absorption spectra of ZnS:La thin films ZnS:La (0- 10%).

Table 1 gives the transmittance (T), the absorption threshold (λ) and the band gap energies (Eg) for the various compositions at room temperature. These values are conforms with the AFM and SEM analyses and this behavior is related to the nanometric size of the particles that is due to the quantum confinement effect [27]. These results are in agreement with those found by other authors [21, 28]. In other case, the decreasing of band gap energy with the composition can be induced to the metallization of the la-doped system.

Table 1. The Absorption threshold, the gap values and the maximum transmittance of ZnS thin films doped with lanthanum (0-10%).

Compositions	Absorption thresholds λ (nm)	Optical Gap E_g (eV)	Maximal Transmittance T_{max} (%)
ZnS:La 0%	337	3.68	75
ZnS:La 2%	335	3.70	77
ZnS:La 4%	447	2.77	57
ZnS:La 6%	451	2.75	66
ZnS:La 8%	452	2.74	68
ZnS:La 10%	455	2.73	67

Conclusion

Zinc sulfide doped terbium ($ZnS:La^{3+}$) with different concentrations (0; 2; 4; 6; 8 and 10%) thin films were deposed on glass substrates by a dip-coater using sol-gel method. X-ray diffraction analysis has revealed that the thin layers for all compositions are amorphous. Atomic force microscopy images of the films have revealed a homogeneous and granular structure. Doping decreases roughness. The optical transmission spectra in the UV - visible range have shown that all the doped films present a good optical transmission in the visible. The calculated values of gap were between 3.70 and 2.73 eV. Analysis FTIR of the powders confirms the presence of the vibration band of Zn-S at 668 cm^{-1}.

References

1. Jin, Q.; Li, Y.; Huo, J.; Zhao, X.; Sensors and Actuators, **2016**, B 227, 108.
   DOI: 10.1016/j.snb.2015.12.036
2. Hasani, M.; Coto García, A.M.; Costa-Fernández, J. M.; Sanz-Medel, A.; Sensors and Actuators B, **2010**, 144, 198.
   DOI: 10.1016/j.snb.2009.10.066
3. Gómez-Barojas, E.; Sánchez-Mora, E.; Castillo-Abriz, C.; Flores-Rodríguez, E.; Silva-González, R.; J. Supercond. Nov. Magn., **2013,** 2337.
   DOI: 10.1007/s10948-012-1432-5
4. Jang, J.S.; Kim, E.S., Choi, S.H.; Kim, D.H., Kim, H.G.; Lee, J.S.; Applied catalysis A, General, **2012**, 427-428,106.
   DOI: 10.1016/j.apcata.2012.03.038
5. Tiwari, G.; Brahme, N.; Sharma, R.; Bisen, D.P.; Sao, S. K.; International Research Journal of Engineering and Technology (IRJET), **2015**, 02(02).
   e-ISSN: 2395 -0056 ; p-ISSN: 2395-0072
6. Sivakami, R.; Thiyagarajan, P.; Nano-Structures & Nano-Objects, **2016**, 6, 59.
   DOI: 10.1016/j.nanoso.2016.03.001
7. Wang, Z.A.; Chu, J.B.; Zhu, H.B.; Sun, Z.; Chen, S Y.W.; Huang, M.; Solid-State Electronics, **2009**, 53, 1149.
   DOI: 10.1016/j.sse.2009.07.006
8. Gopakumar, N.; Anjana, P. S.; Vidyadharan Pillai, P. K., J. Mater. Sci., **2010**, 45, 6653.
   DOI: 10.1007/s10853-010-4756-1
9. Suycano, K. P.; Santos, G. N. C.; Quiroga, R. V.; DLSU Research Congress,**2015**.
   Presented at the DLSU Research Congress 2015
   De La Salle University, Manila, Philippines, March 2-4, 2015
10. Liu, B.; Liu, Q.; Tong, X.; Lü, C.; Colloid. Surf., **2013**, A, 434, 213.
    DOI: 10.1016/j.proeng.2012.03.009
11. Goktas, A.; Aslan, F.; Yasar, E.; Mutlu, I. H.; J. Mater. Sci.: Mater. Electron., **2012,** 1361.
    DOI: 10.1007/s10854-011-0599-z
12. Akhtar, M. S.; Malik, M. A.; Riaz, S.; Naseem, S.; O'Brien, P.; Materials Science in Semiconductor Processing, **2015**, 30, 292.
    DOI: 10.1016/j.mssp.2014.10.019
13. Gayou, V. L.; Salazar-Hernandez, B.; Constantino, M. E.; Andres, E. R.; Dıaz, T.; Macuil, R. D.; Lopez, M. R.; Vacuum, **2010**, 84, 1191.
    DOI: 10.1016/j.vacuum.2009.10.023
14. Cui, J.; Zeng, X.; Zhou, M.; Hu, C.; Zhang, W.; Lu, J.; Journal of Luminescence, **2014**, 147, 310.
    DOI: 10.1016/j.jlumin.2013.11.057
15. Hoa, T. T. Q.; The, N. D.; McVitie, S.; Nam, N. H.; Vu, L. V.; Canh, T.D.; Long , N. N.; Optical Materials, **2011**; 33, 308.
    DOI: 10.1016/j.optmat.2010.09.008
16. Wang, L.; Dai, J.; Liu, X.; Zhu, Z.; Huang, X.; Wu, P. ; Ceramics International, **2012**, 38, 1873.
    DOI: 10.1016/j.ceramint.2011.10.013
17. Mukherjee, A.; Mitra, P.; Journal of Physical Sciences, **2012**, 16,171.
    ISSN: 0972-8791, www.vidyasagar.ac.in/journal
18. Vanbesien, K.; De Visschere, P.; Smet, P.F.; Poelman, D.; Thin Solid Films, **2006**, 514 ,323.
    DOI: 10.1016/j.tsf.2006.02.034
19. Bhargava, R. N.; Gallagher, D.; Hong, X.; Nurmikko, A.; Phys. Rev. Lett., **1994**, 72(3), 416.
20. Liang, Z.; Mu, J.; Han, L.; Yu, H.; Journal of Nanomaterials, **2015,** 1.
    DOI: 10.1155/2015/519303
21. Varughese, G.; Sreeja, R.; Aswathy, S. R.; Usha , K.T.; Kumar, A.S.; Advanced Materials Research, **2013**, 622-623, 752.
    DOI: 10.4028/www.scientific.net/AMR.622-623.752
22. Luque, P. A.; Gómez-Gutiérrez,C. M.; Lastra, G.; Carrillo-Castillo, A.; Quevedo-López, M.A.; Olivas, A.; Jurnal of Electronic Materials, **2014**, 43(11).
    DOI: 10.1007/s11664-014-3334-8
23. Wahab, R.; Ansari, S. G.; Kim, Y.S.; Dhage, M. S.; Seo, H. K.; Song, M.; Shin, H. S.; Met. Mater. Int., **2009**, 15(3), 453.
    DOI: 10.1007/s12540-009-0453-5
24. Bu, I.Y.Y.; Journal of Luminescence, **2013**,134, 423.
    http://dx.doi.org/10.1016/j.jlumin.2012.08.008
25. Reddy, D. A.; Liu, C.; Vijayalakshmi, R.P.; Reddy, B.K.; Journal of Alloys and Compounds, **2014**, 582, 257.
    DOI: 10.1016/j.jallcom.2013.08.051
26. Viswanath, R.; Naik, H. S. B.; Somalanaik, Y. K. G.; Neelanjeneallu, P. K. P.; Harish, K. N.; Prabhakara, M. C.; Journal of Nanotechnology, **2014,** 1.
    DOI: 10.1155/2014/924797
27. Göde, F.; Gümü, C.; Zor, M.; Journal of Crystal Growth, **2007**, 299, 136.
    DOI: 10.1016/j.jcrysgro.2006.10.266
28. Chen, Y.; Huang, G. F.; Huang, W. Q.; Zou, B.S.; Pan, A.; Appl. Phys. A, **2012**, 108, 895.
    DOI: 10.1007/s00339-012-6990-7

